Geobiology

Geobiology (2013), **11**, 406–419 DOI: 10.1111/gbi.12045

Carbon isotopes and lipid biomarkers from organic-rich facies of the Shuram Formation, Sultanate of Oman

C. LEE,[1,2] D. A. FIKE,[3] G. D. LOVE,[1] A. L. SESSIONS,[2] J. P. GROTZINGER,[2] R. E. SUMMONS[4] AND W. W. FISCHER[2]

[1]*Department of Earth Sciences, University of California, Riverside, CA, USA*
[2]*Division of Geological and Planetary Sciences, California Institute of Technology, Pasadena, CA, USA*
[3]*Earth and Planetary Sciences, Washington University St Louis, St. Louis, MO, USA*
[4]*Earth, Atmospheric and Planetary Sciences, Massachusetts Institute of Technology, Cambridge, MA, USA*

ABSTRACT

The largest recorded carbon isotopic excursion in Earth history is observed globally in carbonate rocks of middle Ediacaran age. Known from the Sultanate of Oman as the 'Shuram excursion', this event records a dramatic, systematic shift in $\delta^{13}C_{carbonate}$ values to *ca.* −12‰. Attempts to explain the nature, magnitude and origin of this excursion include (i) a primary signal resulting from the protracted oxidation of a large dissolved organic carbon reservoir in seawater, release of methane from sediment-hosted clathrates, or water column stratification; and (ii) a secondary signal from diagenetic processes. The compositions and isotope ratios of organic carbon phases during the excursion are critical to evaluating these ideas; however, previous work has focused on localities that are low in organic carbon, hindering straightforward interpretation of the observed time-series trends. We report carbon isotope data from bulk organic carbon, extracted bitumen and kerogen, in addition to lipid biomarker data, from a subsurface well drilled on the eastern flank of the South Oman Salt Basin, Sultanate of Oman. This section captures Nafun Group strata through the Ediacaran–Cambrian boundary in the Ara Group and includes an organic-rich, deeper-water facies of the Shuram Formation. Despite the high organic matter contents, the carbon isotopic compositions of carbonates – which record a negative $\delta^{13}C$ isotope excursion similar in shape and magnitude to sections elsewhere in Oman – do not covary with those of organic phases (bulk TOC, bitumen and kerogen). Paired inorganic and organic $\delta^{13}C$ data only display coupled behaviour during the latter part of the excursion's recovery. Furthermore, lipid biomarker data reveal that organic matter composition and source inputs varied stratigraphically, reflecting biological community shifts in non-migrated, syngenetic organic matter deposited during this interval.

Received 28 January 2013; accepted 24 May 2013

Corresponding authors: C. Lee. Tel.: +14242488232; fax: +19518274324; e-mail: clee093@ucr.edu
W. W. Fischer. Tel.: +16263956790; fax: +16265680935; e-mail: wfischer@caltech.edu

INTRODUCTION

The rock record of the late Neoproterozoic Era (*ca.* 800–541 Ma) captures a dynamic time in Earth history, marked by several global low-latitude glaciations (Hoffman *et al.*, 1998), increasing and widespread oxygenation of Earth's atmosphere and oceans (Knoll *et al.*, 1986; Fike *et al.*, 2006; Scott *et al.*, 2008), and the evolution and diversification of Metazoa (Knoll & Carroll, 1999). Subsequent to the Cryogenian global glaciations yet prior to the evolution of bilateria near the Ediacaran–Cambrian boundary, middle Ediacaran-age successions host the largest negative carbon isotopic excursion observed in the geologic record, with values of $\delta^{13}C_{carbonate}$ ($\delta^{13}C_{carb}$) as low as −12‰ (summarised in Grotzinger *et al.*, 2011). This excursion was first observed in the Wonoka Formation of South Australia (Jansyn, 1990; Pell *et al.*, 1993; Urlwin *et al.*, 1993). Burns & Matter (1993) were the first to detail the unusual excursion in Oman and link these carbon cycle dynamics to animal evolution. In addition to Oman (e.g. Le Guerroué *et al.*, 2006a,b,c) and Australia (e.g. Calver, 2000), negative excursions displaying similar characteristics

have been observed in many Ediacaran sedimentary successions, including the Doushantuo Formation of South China (e.g. McFadden *et al.*, 2008) and the Johnnie Formation of the western United States (e.g. Kaufman *et al.*, 2007; Bergmann *et al.*, 2011).

If primary, the striking pattern observed in the Shuram excursion stretches our ability to interpret the historical behaviour of the carbon cycle using commonly applied assumptions in an isotope mass balance framework. Fundamentally, explanations must invoke carbon fluxes into the fluid Earth with isotope ratios lower than commonly assumed for outgassing and weathering. Alternatively, it has been hypothesised that the Shuram excursion does not record the primary isotopic composition of marine dissolved inorganic carbon (DIC), but was caused rather by secondary, diagenetic processes – perhaps global in scope (Bristow & Kennedy, 2008; Knauth & Kennedy, 2009; Derry, 2010a; Grotzinger *et al.*, 2011; Schrag *et al.*, 2013). Several observations fuel diagenetic hypotheses – including the widely observed positive correlation between the carbon and oxygen isotopic composition of carbonates – but another critical part of the Shuram puzzle is that the isotopic composition of coeval organic matter does not record the same time-series pattern, but is instead largely invariant (e.g. Fike *et al.*, 2006; McFadden *et al.*, 2008). This feature might be most simply explained if the excursion were diagenetic in origin (e.g. Derry, 2010b), but two different hypotheses have been developed to explain the pattern as a consequence of primary sedimentary and carbon cycle processes.

Focusing on the pattern of decoupled $\delta^{13}C_{carb}$ and $\delta^{13}C_{org}$ values in Neoproterozoic successions, Rothman *et al.* (2003) formulated a generic carbon cycle scenario in which both the negative excursions in $\delta^{13}C_{carb}$ values and the invariant organic matter $\delta^{13}C$ values ($\delta^{13}C_{org}$) were caused by the slow oxidation of a large dissolved organic carbon (DOC) seawater pool (Rothman *et al.*, 2003). A large DOC reservoir, much larger than the mass of inorganic carbon in DIC, allows $\delta^{13}C_{org}$ to be buffered against isotopic variation, while its progressive and eventual remineralisation would have produced ^{13}C-depleted isotope ratios observed in carbonate (Rothman *et al.*, 2003). Fike *et al.* (2006) subsequently invoked this hypothesis to explain the Shuram excursion, and this idea has seen broad application to explain decoupled carbonate–organic data sets from other sections (e.g. McFadden *et al.*, 2008) and Neoproterozoic intervals (e.g. Swanson-Hysell *et al.*, 2010), and has been integrated into new modelling approaches (Bjerrum & Canfield, 2011). A reasonable concern with the decoupling argument comes from the quality of the organic carbon isotope data, much of which comes from organic-lean sections (Calver, 2000; Fike *et al.*, 2006; Swanson-Hysell *et al.*, 2010) – with TOC wt% values of <0.05, perhaps approaching analytical blanks. Recently, it was proposed that throughout Neoproterozoic time, $\delta^{13}C_{org}$ values should record an expected ^{13}C-depleted linear translation of DIC trends and that the reason organic-lean samples do not recapitulate the expected trends is because the $\delta^{13}C_{org}$ of these samples is instead controlled by admixtures of fossil detrital or migrated organic carbon (Johnston *et al.*, 2012). In order to test these different hypotheses, it is important to examine the isotopic systematics of strata that capture the Shuram excursion that are rich in organic carbon and derived from unweathered materials.

Much of the Shuram Formation studied thus far is organic lean in both outcrop and subsurface strata, but in certain areas of the basin, petroliferous and fossiliferous strata are preserved. The eastern flank of the South Oman Salt Basin (Fig. 1A) contains extremely thermally well-preserved molecular fossils (e.g. Love *et al.*, 2008, 2009; Grosjean *et al.*, 2009) as well as a suite of sphaeromorphic acritarchs and filamentous microfossil assemblages in the Nafun Group (Butterfield & Grotzinger, 2012). Here, we report isotopic and lipid biomarker data from an eastern flank locality that captures a deeper-water (Fig. 1B), organic-rich facies of the Shuram and overlying Buah formations, in order to better understand carbon cycle processes and biological community dynamics through the Shuram excursion.

Geological setting

The Huqf Supergroup of the Sultanate of Oman provides one of the best-preserved, most continuous late Neoproterozoic to early Cambrian (*ca.* 713–540 Ma; Allen, 2007; Bowring *et al.*, 2007) successions globally. Outcrop exposures of Huqf strata are limited to the Oman Mountains in the north, Mirbat area in the south, and the Huqf area, but a substantial amount of knowledge and materials exist from numerous petroleum exploration and production wells throughout the subsurface, particularly the South Oman Salt Basin (Schröder *et al.*, 2004) (Fig. 1).

The Huqf Supergroup is composed of three groups that show broadly similar stratigraphic patterns between the sub-basins. The lowest group – the Abu Mahara – is composed of clastics, including Cryogenian-age, glacially-derived sediments (Allen, 2007). The overlying Nafun Group begins with the Marinoan (*ca.* 630 Ma) Hadash cap carbonate and then records two overall clastic-to-carbonate shallowing upward trends defined by the Masirah Bay clastics and overlying Khufai Formation carbonate ramp, and the Shuram Formation mixed clastics and carbonates with the overlying Buah Formation carbonate ramp (McCarron, 2000; Grotzinger *et al.*, 2002; Cozzi *et al.*, 2004; Le Guerroué *et al.*, 2006a). The Shuram excursion nearly covers one of these first-order cycles, beginning in the

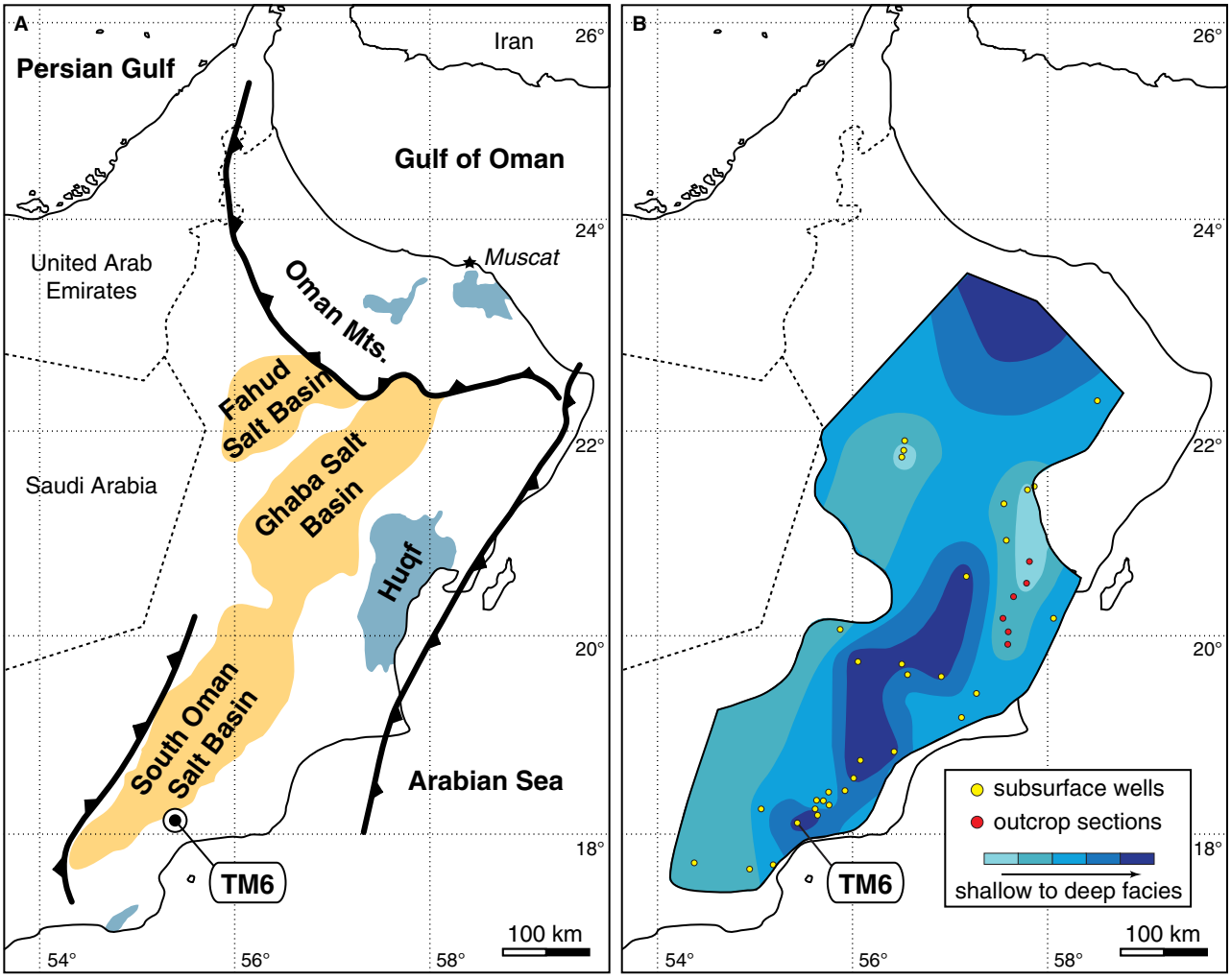

Fig. 1 Left panel: geologic map of the sub-basins containing Huqf Supergroup strata throughout the Sultanate of Oman. Outcrop localities are shown in dark blue; subsurface salt basins are shown in orange. The location of the subsurface well TM-6 on the eastern flank of the South Oman Salt Basin is marked. Right panel: bathymetric facies map of the Shuram Formation in Oman (data from Petroleum Development Oman and Le Guerroué *et al.*, 2006a).

uppermost Khufai Formation (Osburn *et al.*, 2013) with the recovery finishing in the lower Buah Formation (Burns & Matter, 1993; Le Guerroué *et al.*, 2006a). Finally, the Ara Group records an evaporite basin with several successive carbonate platform stringers (Gorin *et al.*, 1982; Schröder *et al.*, 2004). Despite similar overall stratigraphic patterns between basins, facies differences between regions record striking gradients in paleoenvironment; Nafun Group strata exemplify this.

The Shuram Formation exhibits significant facies changes across Oman. In outcrop, it is well known that shallow shelf platform facies in the Huqf outcrop region pass downdip into sub-wave base deposits (McCarron, 2000; Le Guerroué *et al.*, 2006a,b). The depositionally updip deposits include wave-rippled to hummocky cross-stratified siltstones and fine sandstones, interstratified with trough cross-stratified ooid grainstones and intraclast conglomerates. Characteristically these upper shoreface deposits form shallowing-upward cycles in which the siliciclastic-dominated facies pass upward into the carbonate-dominated facies (Le Guerroué *et al.*, 2006b).

In contrast, downdip facies are expressed as interbedded siliciclastic mudstones and siltstones, with zones of carbonate cementation and concretion development. Convolute bedding and slump structures are present, along with current ripples. Uncommonly, small-scale hummocky cross-stratification is observed. References to 'organic-rich' facies in outcrop have been noted (e.g. Le Guerroué *et al.*, 2006a) though these have not been confirmed through measurement of organic carbon concentrations.

Due to the lack of surface oxidative weathering, the subsurface record of Shuram Formation facies variability provides the best indicator of how primary concentrations of organic content vary spatially and temporally throughout

the formation. Well data collected by Petroleum Development Oman over the past 40 years were examined by Le Guerroué *et al.* (2006a) who reproduced their facies map for the Shuram Formation (Fig. 1B). Figure 1B shows these lateral facies changes in the Shuram, illustrating the presence of deeper-water facies trending NE–SW, shallowing to the east along the Huqf area outcrop belt, a long-lived topographic high. The western limit of the deeper-water facies belt is uncertain due to uplift and erosion along the Western Deformation Front (Loosveld *et al.*, 1996; Grotzinger *et al.*, 2002). Paleogeographic trends suggest it would have continued to deepen in a westerly direction (see Allen, 2007, Fig. 10).

Only a small fraction of the Shuram Formation has been cored. Fortunately, it is standard industry practice to analyse cuttings for information regarding lithology, including primary sedimentology, diagenesis and the detection of organic-rich facies. Wireline logs additionally provide a wealth of petrophysical data that can provide important constraints on organic content. The presence of organic matter can be confidently detected with a combination of increasing gamma ray values, sonic transit time, neutron porosity and resistivity, and with reduction in the formation bulk density (Meyer & Nederlof, 1984; Mann *et al.*, 1986; Herron & Le Tendre, 1990). Based on analysis of wireline logs and organic geochemical analyses of cuttings, the Shuram Formation was recognised to contain organic-rich source rocks in deeper-water paleogeographic settings (Le Guerroué *et al.*, 2006a; Grosjean *et al.*, 2009). We examined materials from the TM-6 well located within this organic-rich, deeper-water facies belt (Fig. 1B).

METHODS

Sample preparation and bitumen extraction

Samples from TM-6, collected as cm-sized drill cuttings, were initially soaked and rinsed 3× in distilled deionised (DI) water, then rinsed with 3× methanol, 3× dichloromethane and 3× *n*-hexane to remove residual surface contamination. The cuttings were milled to fine powder using a SPEX 8510 Shatterbox with an alumina ceramic container.

Rock powders (typically 1.5–3 g) were extracted in 20 mL of dichloromethane:methanol (9:1 v/v) (CEM MarsXpress) at 100 °C for 15 min with constant stirring. One blank consisting of pre-baked silica sand was extracted with each batch of samples. After cooling, sample extracts were filtered and solvent was evaporated under a stream of pure N_2 into pre-tared vials. To ensure complete extraction, the remaining sediment was re-extracted – up to eight times – until the extract contained no more measurable (by weight) bitumen.

Kerogen isolation and Total Organic Carbon (TOC)

To isolate kerogen, solvent-extracted rock powder was acidified at room temperature using concentrated hydrochloric acid (1 N) for 48 h to remove carbonate minerals. The powders were rinsed repeatedly with DI water until a pH range of 4–5 was achieved. To prepare samples for TOC measurements, whole-rock power was acidified as described above. Samples were dried overnight and loaded into capsules for analysis.

Isotope ratio analyses

Carbonates

Carbonate carbon ($\delta^{13}C_{carb}$) and oxygen isotopes ($\delta^{18}O_{carb}$) were measured on CO_2 after reaction with anhydrous phosphoric acid by gas-source mass spectrometry according to standard methods previously described in Ostermann & Curry (2000). Data are reported in the conventional $\delta^{13}C$ notation as parts per thousand (permil) deviations from the VPDB standard. The sulphur isotopic composition of carbonate-associated sulphate (CAS) was determined by dissolution of carbonate and precipitation of barite, followed by combustion to SO_2 and analysis by gas-source mass spectrometry; the details of the method are outlined in Fike & Grotzinger (2008). Briefly, CAS was obtained by dissolving powered sample in 6 N HCl for either 2 h at 60 °C under nitrogen gas or 12–24 h at room temperature. Samples were filtered to eliminate insoluble residues, and excess barium chloride was added to the filtrate to precipitate barium sulphate for subsequent analysis. Sulphur isotope ratio data are reported in permil relative to the VCDT standard. Samples were calibrated using the international standards NBS-127 (20.3‰) and S3 (−31.5‰), as well as four internal standards: silver sulphide (ERE-Ag_2S: −4.3‰), chalcopyrite (EMR-CP: 0.9‰) and two barium sulphate standards (BB4-18: 39.5‰; PQB: 38.0‰) (Fike & Grotzinger, 2008).

Organics

TOC and kerogen fractions were loaded into tin capsules (Costech) as powder. Bitumen dissolved in dichloromethane was pipetted into tin capsules and the solvent was evaporated to dryness prior to analysis. Samples for bitumen and kerogen were flash-combusted in a 1000 °C furnace using a Costech Analytical Technologies Elemental Analyser (EA). The resulting CO_2 gas was analysed by continuous flow using a Delta-S Isotope Ratio Mass Spectrometer (IRMS). Samples for TOC were flash-combusted at 1060 °C in a Carlo Erba NA1500 Elemental Analyser fitted with an AS200 autosampler. The resulting CO_2 gas was analysed by a Delta-plus XP IRMS. Organic carbon isotope ratios are reported in the conventional delta

notation as permil variations relative to the VPDB standard. Calibration of $\delta^{13}C_{org}$ values was accomplished by comparison with system blanks (empty tin capsules) and two working standards: acetanilide ($C_6H_5NH(COCH_3)$) and urea (CH_4N_2O). Blanks and standards were run after every ten sample measurements. Sample $\delta^{13}C$ values were repeatable to a standard error of 0.26‰ (TOC), 0.32‰ (bitumen) and 0.54‰ (kerogen). Standards were repeatable to a standard error of 0.08‰ (acetanilide standard; $n = 20$) and 0.06‰ (urea standard; $n = 23$).

Lipid biomarkers

Traces of elemental sulphur were removed from bitumen extracts using activated copper turnings. The extract was separated into three fractions by columns filled with dry-packed silica gel. The saturates fraction was eluted with *n*-hexane, the aromatics with *n*-hexane:dichloromethane (4:1 v/v) and the polars with dichloromethane:methanol (3:1 v/v). A deuterated C_{29} sterane standard (d4-ααα-24-ethylcholestane (20R), Chiron Laboratories AS) was added to the saturate fraction prior to biomarker quantification through GC-MS. Typically, 50 ng of internal standard was added to a 1-mg aliquot of saturates.

Gas Chromatography–Mass Spectrometry (GC-MS) and Multiple Reaction Monitoring (MRM)

Saturated hydrocarbons were analysed by gas chromatography–mass spectrometry (GC-MS) in full scan mode on a Micromass Autospec Ultima equipped with a HP6890 gas chromatograph (Hewlett Packard). Sterane and hopane biomarkers were analysed on the Autospec instrument by multiple reaction monitoring (MRM). Details of the run conditions and uncertainties in the biomarker ratios are the same as in Love *et al.*, 2009. Uncertainties in polycyclic biomarker ratios determined from multiple analyses of a saturated hydrocarbon fraction from AGSO standard oil are ±8%.

RESULTS AND DISCUSSION

Figure 2 contains a compilation of geochemical and isotope ratio profiles spanning *ca.* 1000 m of the Huqf Supergroup strata, ranging from the lower Masirah Bay siliciclastics into Ara Group carbonates. $\delta^{13}C_{carb}$ values display two well-defined negative excursions (Fig. 2B). The first begins near the contact of the Khufai and Shuram formations, with $\delta^{13}C_{carb}$ values dropping from +5‰

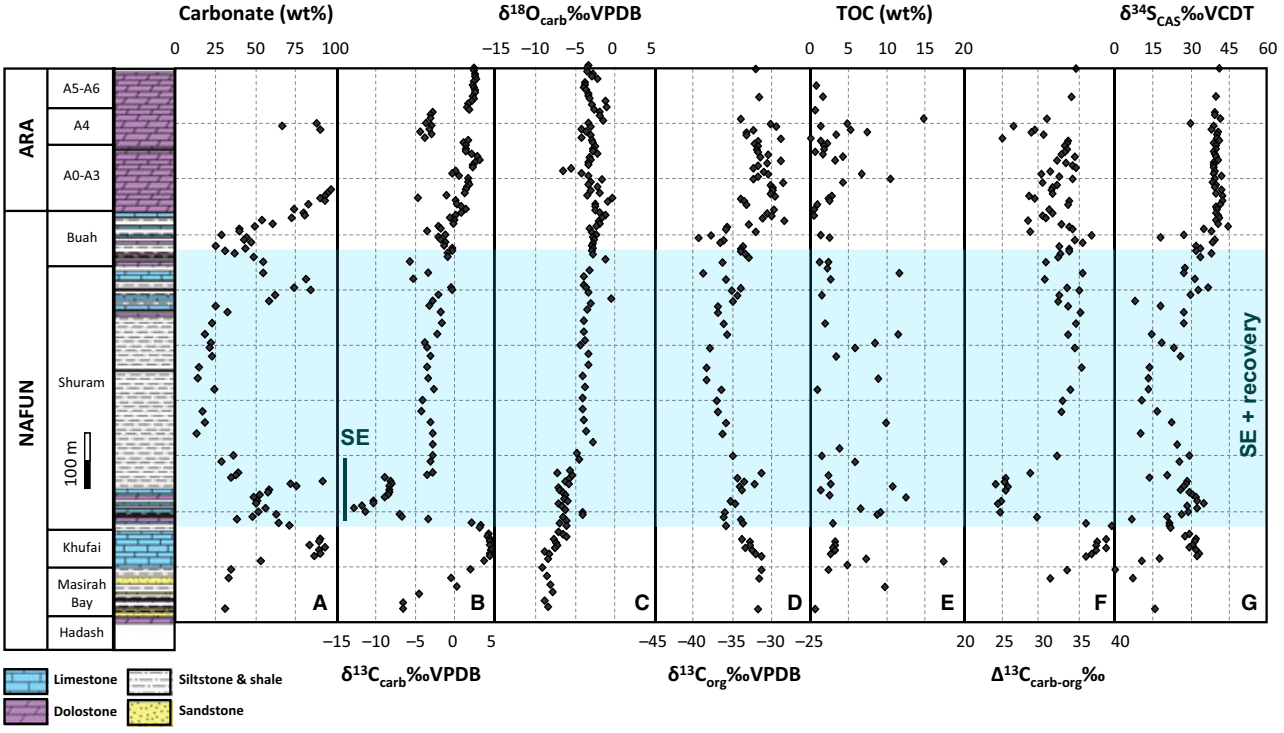

Fig. 2 Isotopic and geochemical profiles from TM-6 plotted alongside stratigraphy. Lithologic log and group and formation names are plotted along the left. (A) Carbonate content measured in weight per cent (wt%). Note that well cuttings mix the interbedded siliciclastic and carbonate lithologies typical of the Shuram Formation. (B) Carbon isotopic composition of carbonate, both dolomite and limestone in ‰ VPDB. (C) Oxygen isotopic composition of carbonate in ‰VPDB. (D) Carbon isotopic composition of bulk organic carbon in ‰VPDB. (E) Total organic carbon content measured in weight per cent (wt%). (F) $\Delta_{carb\text{-}org}$, calculated as the difference between $\delta^{13}C_{carb}$ and $\delta^{13}C_{org}$ values in ‰VPDB. (G) Sulphur isotopic composition of carbonate associated sulphate (CAS) in ‰VCDT. Pale blue shaded panel indicates the Shuram excursion (SE) and recovery; the line in panel B represents the +5‰ to −12‰ excursion.

to −12‰ over *ca*. 70 m of stratigraphy with the recovery taking place over the overlying *ca*. 400 m into the Buah Formation. Even in this deeper depositional environment with far higher sedimentary organic carbon loadings, this $\delta^{13}C_{carb}$ excursion is very similar in shape and magnitude to the observations presented in Burns & Matter (1993), and elsewhere in Oman (Fike *et al*., 2006; Le Guerroué *et al*., 2006a,c). A second excursion occurs stepwise in the A4 unit of the Ara Group, is smaller in magnitude and has been interpreted to mark the Ediacaran–Cambrian boundary at 541 Ma (Amthor *et al*., 2003; Schröder *et al*., 2004; Bowring *et al*., 2007). Both carbonate carbon isotope excursions do not correlate with wt% carbonate (Figs 2A,B and 5B).

$\delta^{18}O_{carb}$ reveals a wide range of values (from 0 to −9‰) characteristic of differential alteration during carbonate diagenesis (Fig. 2C). $\delta^{18}O_{carb}$ values generally decline with stratigraphic depth, suggesting carbonate recrystallisation during burial, although this interpretation is non-unique without independent constraints on recrystallisation temperatures or fluid compositions. It is notable, however, that we do not observe the strong covariation of ^{13}C and ^{18}O isotope ratios in carbonates observed elsewhere in Oman through the Shuram excursion (e.g. Burns & Matter, 1993; Fike *et al*., 2006; Fike, 2007), similar to observations from Le Guerroué & Cozzi (2010) and potentially other correlative sections (e.g. Bergmann *et al*., 2011; Loyd *et al*., 2013). This result suggests the operation of a different combination of diagenetic processes in the carbonates deposited in this deeper-water paleoenvironment and is not readily explained by existing diagenetic hypotheses for the Shuram carbon isotope excursion (e.g. Bristow & Kennedy, 2008; Knauth & Kennedy, 2009; Derry, 2010a).

Bulk organic carbon isotope ratios ($\delta^{13}C_{org}$) (Fig. 2D) show a wide range of values from −28 to −39‰, and several systematic trends within the stratigraphy. A broad negative excursion covers much of the Nafun Group strata, beginning in the lower Khufai Formation and ending at the top of the Buah Formation. Superimposed on this trend is a smaller positive excursion in the lower Shuram Formation. Neither $\delta^{13}C_{org}$ or $\delta^{13}C_{carb}$ data show significant relationships with organic carbon concentrations (TOC wt%) ($\delta^{13}C_{org}$ $m = -1.6$, $R^2 = 0.05$ and $\delta^{13}C_{carb}$ Fig. 5D), which are generally high throughout the stratigraphy (4.4 ± 3.8 wt%; Fig. 2E).

The trends observed in $\delta^{13}C_{org}$ do not directly mirror those of $\delta^{13}C_{carb}$ (Fig. 5C). The fractionation between carbonate and organic carbon ($\Delta_{carb\text{-}org}$; Fig. 2F) is not constant, but rather exhibits a clear systematic pattern that mimics the Shuram excursion. Typical average marine values during the last 800 Ma for $\Delta^{13}_{carb\text{-}org}$ are in the range of 28–32‰ (Hayes *et al*., 1999; Ader *et al*., 2009). $\Delta_{carb\text{-}org}$ values from TM-6 show a range between 24 and 39‰ and an average value of 32 ± 3.5‰. During the nadir of the Shuram excursion, $\Delta_{carb\text{-}org}$ values are 25 ± 0.6‰, whereas from the middle Shuram to upper Buah and A4 units in the Ara, average $\Delta_{carb\text{-}org}$ values are 33 ± 1.9‰. Finally, we do not observe the relationship between $\Delta_{carb\text{-}org}$ and TOC values hypothesised by Johnston *et al*. (2012).

The sulphur isotopic composition of carbonate-associated sulphate ($\delta^{34}S_{CAS}$) shows an overall general positive trend from a nadir in the middle Shuram Formation to high $\delta^{34}S$ values (to 40‰) in the Ara Group (Fig. 2G), observed throughout Oman (Fike & Grotzinger, 2008). The lower Nafun Group strata reveal high $\delta^{34}S_{CAS}$ values in the lower Khufai Formation, which subsequently drop by approximately 10‰, reversing course briefly with a small positive trend at the onset of the Shuram excursion. Superimposed on these trends are ^{34}S-depleted values that stand out from the trend and might reflect alteration by secondary processes (Fike & Grotzinger, 2008), possibly including contamination by coexisting pyrite during CAS extraction (e.g. Marenco *et al*., 2008). Overall, the $\delta^{34}S_{CAS}$ trends associated with the Shuram excursion in TM-6 are similar to those observed by Fike *et al*. (2006) from shallower paleoenvironments north of the Huqf area.

Organic geochemical data through the Shuram excursion in TM-6 show a range of features typical of the Huqf Supergroup throughout Oman. Characteristic features of organic matter from source rocks throughout the Huqf Supergroup include conspicuous ^{13}C-depletions ($\delta^{13}C$ *ca*. −36‰), high sulphur content, low pristane/phytane, high relative abundance of C_{29} steranes, lack of rearranged diasteranes, presence of 24-isopropylcholestane and an abundant series of mid-chain methylalkanes – sometimes termed X-peak compounds (Grantham *et al*., 1987; Höld *et al*., 1999; Love *et al*., 2008; Grosjean *et al*., 2009). Oils, in particular from the Eastern Flank Play, have wide ranges of densities (generally high) and viscosities, and crudes exhibit very low gas/oil ratios (Al-Marjeby & Nash, 1986). Oils with the same properties and of similar age are also known from successions in Pakistan, Eastern Siberia, India and the Eastern European Platform (Höld *et al*., 1999). In TM-6, bitumen and kerogen extracted from whole-rock powder have similar $\delta^{13}C$ values and show comparable $\delta^{13}C$ trends with stratigraphic height (Fig. 3A). Kerogen, in general, is slightly ^{13}C-depleted relative to coexisting bitumen (Fig. 3A) in Nafun Group samples – a feature observed in Neoproterozoic-age strata globally, but largely reversed by late Ediacaran time (Logan *et al*., 1995; Höld *et al*., 1999; Kelly, 2009). The largest fractionation between bitumen and kerogen is 6.3‰ and occurs in the middle of the Shuram Formation, whereas latest Ediacaran and early Cambrian samples from the Ara Group show similar values for bitumen and kerogen (within the reproducibility). In general, the carbon isotopic composition of bitumen and

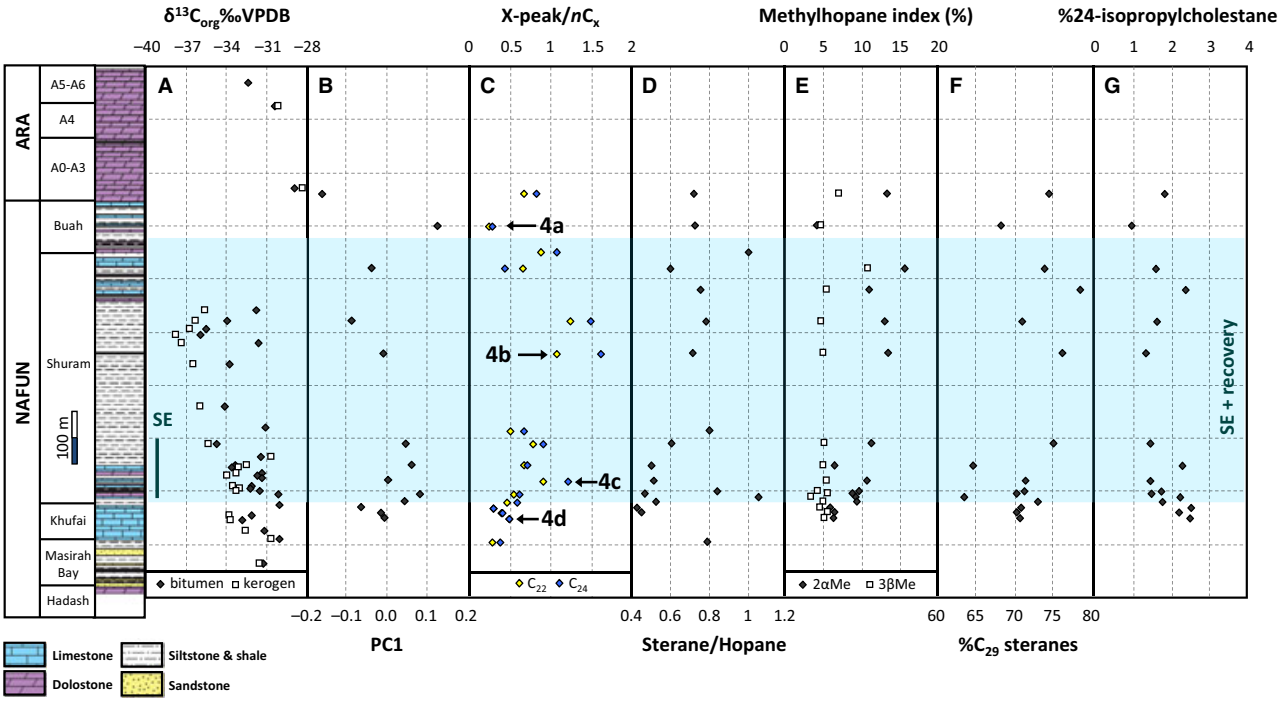

Fig. 3 Carbon isotopic and lipid biomarker stratigraphic profiles from the TM-6 drill well. (A) $\delta^{13}C_{org}$ values for bitumen (filled diamonds) and kerogen (open squares). (B) First principle component (PC1) from principal component analysis of C_{19}-C_{26} *n*-alkane abundances. PC1 explains 91% of the variance in the data set; variable loadings are C_{19} (0.6328), C_{20} (0.3610), C_{21} (0.2050), C_{22} (0.0446), C_{23} (−0.1698), C_{24} (−0.2820), C_{25} (−0.3537), C_{26} (−0.4379). (C) Relative X-peak mid-chain methylalkane abundances measured by X-peak/*n*-alkane for C_{22} (yellow) and C_{24} (blue) homologues. (D) Sterane/hopane (using 2 isomers of diasteranes and 4 isomers of C_{27}-C_{29} regular steranes/19 isomers of C_{27}-C_{35} hopanes; Cao *et al.*, 2009). (E) Methylhopane indices for 2α-methylhopane (filled diamonds) [(2-methyl C_{30} hopane/2-methyl C_{30} hopane + C_{30} αβ hopane) × 100)] and 3β-methylhopane (open squares) [C_{31} 3β-methylhopane/(C_{30} αβ methylhopane + C_{31} 3β-methylhopane) × 100]. (F) Relative abundance of C_{29} steranes to total C_{27}-C_{29} steranes, in per cent (4 isomers of C_{29} regular steranes/4 isomers of C_{27}-C_{29} regular steranes × 100). (G) Relative abundance of 24-isopropylcholestane to total C_{27}-C_{29} steranes, in per cent (24-isopropylcholestane/2 isomers of diasterane and 4 isomers of C_{27}-C_{29} regular steranes × 100). Pale blue shaded panel indicates the Shuram excursion (SE) and recovery; the line in panel A represents the +5‰ to −12‰ excursion.

kerogen shows a very similar trend to the bulk organic carbon values (Fig. 2D); neither tracks the negative carbon isotope excursion observed in carbonates (Fig. 2B).

Lipid biomarker data from TM-6 bitumens exhibit characteristics similar to Nafun strata and oils studied in TM-6 and elsewhere in Oman (e.g. Grosjean *et al.*, 2009; Love *et al.*, 2009), but also show intraformational differences and trends with stratigraphic height. The abundances of C_{19}-C_{26} *n*-alkanes provide insight into bacterial vs. eukaryotic contributions to sedimentary organic matter. These larger alkanes are not strongly affected by evaporative losses during sample handling, and although they can be modified by biodegradation, this process did not substantially impact the biomarker composition of pre-salt oils (Grosjean *et al.*, 2009). The relative abundances of C_{19}-C_{26} *n*-alkanes, statistically reduced to the first principle component (which explains 91% of the data variance) using principle component analysis, highlight fundamental differences in the organics preserved within the stratigraphy (Fig. 3B). The low-molecular-weight end of the spectrum receives strong positive loadings on PC1, whereas the higher-molecular-weight alkanes receive negative loadings. Consequently, decreasing PC1 values imply greater contributions of algal biomass to sedimentary organic matter – an inference weakly supported by sterane to hopane ratio data (discussed below).

X-peaks are an unusual series of C_{14}-C_{30} mid-chain monomethyl branched alkanes, but with greatest abundance in the C_{20}-C_{26} range, which have been detected before in Huqf oils and sedimentary rocks (Klomp, 1986; Höld *et al.*, 1999; Grosjean *et al.*, 2009) as well as in other late Proterozoic–early Cambrian samples. These include heavy petroleum from Pakistan (Grantham *et al.*, 1987), source rocks and oils from the Eastern European (Russian) Platform (Bazhenova & Arefiev, 1996) and oils from the Eastern Siberian Platform (Fowler & Douglas, 1987). Ratios of mid-chain monomethyl-branched alkanes to *n*-alkanes (*n*-C_x) show very high values throughout the Nafun and Ara groups and several systematic excursions with local maxima recorded in the lower and middle Shuram Formation and local minima in the middle Buah Formation, respectively (Figs 3C and 4). In general,

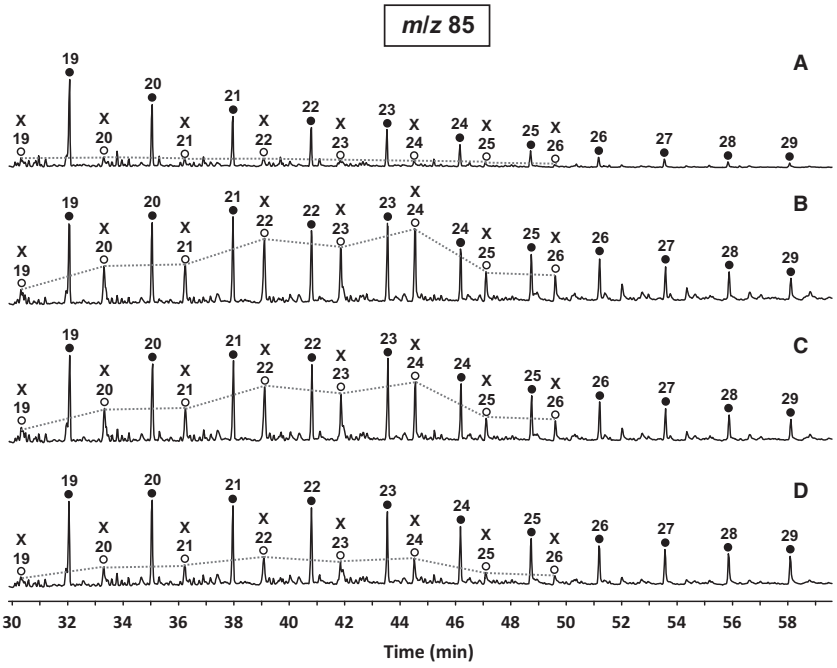

Fig. 4 Selected partial *m/z* 85 ion chromatograms of *n*-alkanes (filled circles) and mid-chain monomethyl alkane series (X-peak compounds; open circles) denoted by their respective carbon numbers through the Shuram excursion. X-peak/nC_x ratios were calculated by integration in *m/z* 85 chromatograms for compounds of the same carbon number (e.g. X-24/nC_{24}). Each chromatogram is labelled with a letter corresponding to their relative stratigraphic position displayed in Fig. 3C. The horizontal axis represents elution time (in minutes), and the vertical axis is relative intensity.

mid-chain monomethyl branched alkane compounds are much less abundant (ratios <0.1 relative to *n*-alkane with the same carbon number) in Phanerozoic rocks (Peters *et al.*, 2005). However, the observation of the C_{20}-C_{26} pattern (X-peaks) with a slight even-over-odd carbon number preference is only prominent in late Neoproterozoic- to early Cambrian-age sedimentary rocks and oils (Love *et al.*, 2008). For typical Phanerozoic strata, the methylalkane abundance tracks *n*-alkane abundance, where small amounts of methylalkanes are partially derived from diagenesis of linear alkanes. Patterns in late Neoproterozoic and early Cambrian samples with prominent X-peaks do not simply record *n*-alkane abundance patterns (Figs 3B,C and 4), implying a specific and significant biological source input for these compounds. The biological sources of X-peak compounds remain unconfirmed at present. Although rare, elevated concentrations of mid-chain monomethyl branched alkanes are observed in unusually organic sulphur-rich Jurassic rocks (e.g. van Kaam-Peters & Sinninghe Damsté, 1997) and suggest these compounds might be derived from organisms living in benthic microbial mats associated with stratified bottom waters, perhaps sulphur-oxidising chemoautotrophic bacteria (Love *et al.*, 2008). If correct, this implies a substantial contribution to sedimentary organic matter from organisms that would have fractionated carbon isotopes quite differently than expectations from ribulose-1,5-bisphosphate carboxylase oxygenase in the Calvin–Benson–Bassham cycle of embryophytes (e.g. Scott *et al.*, 2004). Compound-specific measurements of X-peak compounds reveal a ^{13}C-depletion by an average of 3.7‰ (up to 6.5‰ for C_{24}) when compared to *n*-alkanes in Huqf bitumens (Höld *et al.*, 1999), implying that the source organisms either fractionated carbon isotopes to a greater degree or were benthic and consumed ^{13}C-depleted bottom water DIC (Love *et al.*, 2008). X-peak/*n*-C_x ratios correlate with the $\delta^{13}C$ values of bulk organic carbon, kerogen and to a lesser degree, bitumen. It is interesting, however, that they do not correlate well with $\Delta^{13}_{\text{carb-org}}$. Uncertainty about sources aside, the high X-peak abundances observed in TM-6 strata (up to 60% more abundant than the similar *n*-alkane) are exotic and imply a specific and significant source input. These data also highlight the ever more apparent prevalence of these compounds in the late Neoproterozoic stratigraphic record globally.

Sterane (C_{27}-C_{29}) to hopane (C_{27}-C_{35}) ratios provide a coarse proxy for the relative contributions of bacterial and eukaryotic biomass to preserved sedimentary organic matter. Generally, sterane/hopane ratios increase upsection, but also show significant variability with several notable outliers at the top of the Masirah Bay Formation and within the lower Shuram Formation (Fig. 3D). The ranges in sterane/hopane ratios observed here (between *ca.* 0.4 and 1) imply significant changes in the autotrophic communities through the Shuram excursion, which coincide with the facies and environmental changes observed upsection. These values still remain within the second quartile of the typical range (0.5–2.0) observed in Phanerozoic marine sedimentary rocks and oils (Peters *et al.*, 2005). Although bacteria and eukaryotes can fractionate carbon isotopes differently (due to differences in cell size and physiology; as discussed in Close *et al.*, 2011), we do not

observe relationships between sterane/hopane and the isotopic composition of total organic carbon, bitumen, kerogen or $\Delta^{13}_{carb\text{-}org}$.

Methylhopane indices show stratigraphic variability through the Shuram excursion. 2α-methylhopane indices, describing the relative abundance of compounds largely derived from cyanobacteria and α-proteobacteria (Summons *et al.*, 1999; Welander *et al.*, 2010), vary with depth, but are high throughout much of TM-6 and can exceed 15% (Fig. 3E). These values are consistent with previous observations of microfossils and lipid biomarkers from Proterozoic strata that suggest overall proportionally higher amounts of primary production from bacteria during Neoproterozoic time than is observed from the late Paleozoic through today (Summons *et al.*, 1999; Knoll *et al.*, 2007). The relative abundance of 3β-methylhopanes, compounds largely produced by microaerophilic type 1 methanotrophic proteobacteria and acetic acid bacteria (Farrimond *et al.*, 2004), also vary with depth exhibiting similar overall pattern to 2α-methylhopanes. Despite the stratigraphic variability, the lack of a major secular change in the relative abundance of methylhopanes through the Shuram excursion suggests the absence of extreme temporal shifts in local environmental conditions, for example temperature, salinity, and sedimentary methane fluxes (Rohrssen *et al.*, 2013).

Sterane patterns in TM-6 bitumens are dominated by C_{29} isomers (relative abundances of >70%; Fig. 3F), hydrocarbons derived from sterols typical of green algae (Volkman, 1986). This feature is also characteristic of Proterozoic and Paleozoic bitumens and supports the notion that green algae were important primary producers prior to the Mesozoic marine revolution of higher order endosymbiotic clades (e.g. Grantham & Wakefield, 1988; Schwark & Empt, 2006; Knoll *et al.*, 2007). These observations may also provide some additional context into the possible taxonomic identities of the leiosphaerid acritarchs observed throughout Nafun Group strata (Butterfield & Grotzinger, 2012).

Finally, we observe variable but significant abundances of 24-isopropylcholestanes (from 1 to 3% of summed C_{27}-C_{29} abundances, typical for South Oman oils and rocks) throughout the Nafun Group and Ara Group stratigraphy (Fig. 3G). These biomarkers are thought to reflect the diagenetically stabilised equivalents of C_{30} sterols produced by marine demosponges, and extend into the Cryogenian-age Abu Mahara Group elsewhere in Oman, constituting the oldest observations of Metazoa (Love *et al.*, 2009). From comparative biology, it was recognised that early sponges had an aerobic metabolism (e.g. Berkner & Marshall, 1965; Towe, 1970; King *et al.*, 2008) – anaerobic metazoans appear evolutionarily derived (Danovaro *et al.*, 2010). The facies and source-rock characteristics of this deep-water paleoenvironment suggest that the seafloor in this sub-basin was anoxic through much of Nafun Group time. If 24-isopropylcholestanes were produced by adult benthic organisms with similar growth habits and ecology to modern demosponges (e.g. Sperling *et al.*, 2011), then these molecules were likely advected to deeper sites from organisms living on the shelf. Alternatively, these observations could be explained by the broadcast spawning of planktonic larval stages or an early-evolved sponge group with a largely planktonic life cycle. If the latter is correct, the sedimentary context observed here provides some support for the hypothesis that the evolution and development of sponge larvae may have been an important waypoint in the evolution of higher metazoan taxa (Nielsen, 2008).

IMPLICATIONS FOR CARBON CYCLE FUNCTION THROUGH THE SHURAM EXCURSION

The Shuram excursion presents a suite of challenges to our understanding of the limits of the operation of the Neoproterozoic carbon cycle. This has engendered hypotheses that range from the existence of a large DOC reservoir (Rothman *et al.*, 2003; Fike *et al.*, 2006), to the alteration *via* known (Knauth & Kennedy, 2009; Derry, 2010a; Schrag *et al.*, 2013) and unknown (Grotzinger *et al.*, 2011) diagenetic processes. Though diagenetic hypotheses for the Shuram excursion provide a simple explanation for decoupled carbonate and organic carbon isotope records, we do not observe the covariation of ^{13}C and ^{18}O isotope ratios in TM-6 carbonates through the Shuram excursion (Fig. 5A) anticipated by these diagenetic hypotheses (Knauth & Kennedy, 2009; Derry, 2010a). Although both the absolute values and variation seen in $\delta^{18}O$ throughout the section point to significant water–rock interaction, this alteration does not appear to have significantly affected the $\delta^{13}C$ isotope composition. It is also important to note that the overall magnitude and shape of the Shuram excursion are the same across Oman – from TM-6 in the south to the Huqf area to the Oman Mountains (Burns & Matter, 1993; Le Guerroué *et al.*, 2006c) – despite the dramatic differences in depositional environment (e.g. water depth), sedimentary organic carbon input and burial history between these regions. The differences in burial history of Huqf strata across Oman are substantial; this is suggested by the varying $\delta^{18}O_{carb}$ values across Oman, but not reflected in the $\delta^{13}C_{carb}$ values (Burns & Matter, 1993; Le Guerroué *et al.*, 2006c). This pattern is inconsistent with burial diagenesis hypotheses for the $\delta^{13}C_{carb}$ excursion (e.g. Derry, 2010a). Further, it was recently hypothesised that the Shuram excursion (and the Neoproterozoic carbon isotope record more broadly) reflects the local influence of DIC and alkalinity derived from anaerobic respiration metabo-

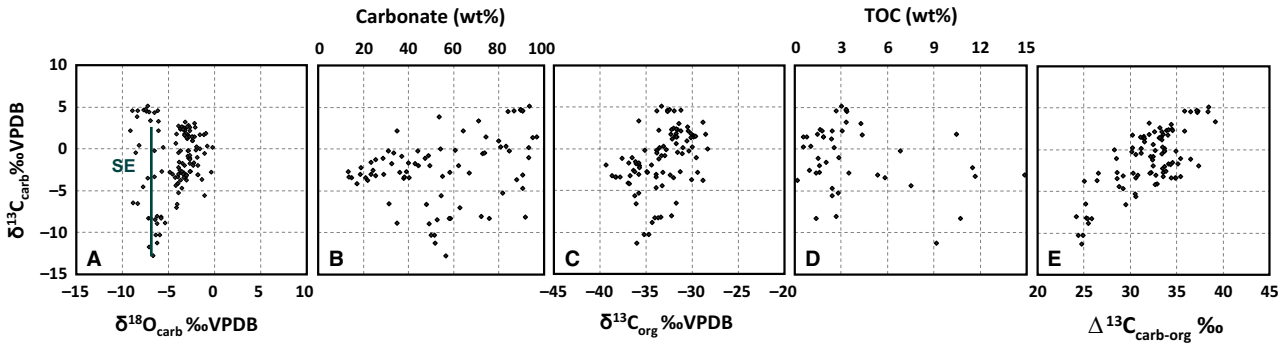

Fig. 5 TM-6 carbonate carbon isotope ratio ($\delta^{13}C_{carb}$) cross-plots plotted against (A) Carbonate oxygen isotope ratios ($\delta^{18}O_{carb}$ ‰VPDB); $R^2 = 0.2$ for data points through the Shuram excursion as indicated. (B) Carbonate abundance in wt%; $R^2 = 0.09$. (C) Organic carbon isotope ratios ($\delta^{13}C_{org}$); $R^2 = 0.2$. (D) Total organic carbon in wt%; $R^2 = 0.08$. (E) $\Delta^{13}C_{carb\text{-}org}$ ‰. The only significant relationship in the cross-plots shown occurs in panel E ($R^2 = 0.55$).

lisms driven by the biological pump and sedimentary organic matter inputs (Schrag *et al.*, 2013). We note that despite the high sedimentary organic carbon loadings present in this part of the basin (which is markedly different than other Oman sections; e.g. Fike *et al.*, 2006), the $\delta^{13}C_{carb}$ excursion is similar (Fig. 5D) – observations that do not support the hypothesis of Schrag *et al.* (2013) for the Shuram excursion. For these reasons, we tentatively regard the carbonate carbon isotope excursion as representative of the time-varying behaviour of marine DIC.

Examining the time series of $\Delta_{carb\text{-}org}$, it is clear that during the onset of the Shuram excursion, carbonate and organic phases were decoupled with regard to their isotopic composition (Fig. 2F). However, from the middle Shuram Formation through the Buah Formation and into the Ara Group – through the latter part of the Shuram excursion recovery – $\delta^{13}C_{carb}$ and $\delta^{13}C_{org}$ show coupled behaviour (Fig. 2F). This is similar to shallower sections in Oman (Fike *et al.*, 2006) and was also observed in Doushantuo unit IV sections from South China (McFadden *et al.*, 2008). These observations (including organic carbon isotope ratios as low as −39‰) support the idea that the Shuram excursion records a primary carbon cycle signal, as the stratigraphic coherence of this covariation is unlikely to occur simply by chance. In general, the disparity between the paired inorganic and organic data sets has been a focal point for hypotheses regarding the nature of Neoproterozoic sedimentary organic matter, suggesting that organic matter could be low in concentration (Jiang *et al.*, 2012; Johnston *et al.*, 2012), buffered by a large, metastable, DOC reservoir (Rothman *et al.*, 2003), or have mixed (Melim *et al.*, 2004; Swart, 2008), multiple (Oehlert *et al.*, 2012) or exogenous (Kaufman *et al.*, 2007; Johnston *et al.*, 2012) carbon sources.

Lipid biomarker and bitumen data from TM-6 support hypotheses that the bulk isotopic composition of sedimentary organic matter reflects multiple syngenetic sources. Organic matter composition and source inputs show stratigraphic variation through the Shuram excursion. In addition, the carbon isotopic composition of kerogen and bitumen display remarkably similar stratigraphic patterns. This discounts hypotheses wherein the organic matter was derived from either a large isotopically homogenous DOC reservoir (e.g. Rothman *et al.*, 2003) or exogenous, migrated or detrital fossil carbon sources. The isotopic compositions of organic phases (bitumen and kerogen) from TM-6 vary stratigraphically, but not as a function of organic carbon concentrations. Furthermore, the difference between $\delta^{13}C_{carb}$ and $\delta^{13}C_{org}$ (here $\Delta_{carb\text{-}org}$, Fig. 2F) does not vary as a function of organic carbon content (TOC wt %) – two variables that Johnston *et al.* (2012) hypothesised should show a hyperbolic relationship due to compositional mixing of syngenetic and fossil detrital organic carbon sources in sections with decoupled carbonate–organic records. Thus, we can effectively rule out the hypotheses that specify inputs from weathering of fossil detrital carbon sources (Kaufman *et al.*, 2007; Johnston *et al.*, 2012) to explain this excursion.

Strong evidence for non-migrated, syngenetic organic matter is demonstrated by two critical observations. First, we report a combination of variable magnitude and distinctive biomarker characteristics (e.g. abundance of distinct X-peak mid-chain methylalkane series and high C_{29} (green algal) and C_{30} (marine demosponge) steranes) in TM-6 samples, as found in all Huqf Supergroup oils and rocks from the South Oman Salt Basin. Similar compositional characteristics were observed from late Neoproterozoic-age eastern Siberian oils (Kelly *et al.*, 2011). Second, the strong relationship between bitumen and kerogen is observed compositionally through comparisons between bitumen and kerogen hydropyrolysates (Love *et al.*, 2008, 2009; Grosjean *et al.*, 2009). This is also reflected in the similarity of their $\delta^{13}C$ values ($m = 1.1$; $R^2 = 0.61$), which is congruent with non-migrated marine-derived organic matter.

Models of the Neoproterozoic carbon cycle that predict the isotopic composition of sedimentary organic matter as a linear translation of carbonate carbon isotope time-series data probably are too simple to accurately describe the carbon cycling at this time, particularly during large perturbations. Organic carbon isotope ratios need not provide a global proxy and can show idiosyncratic local differences depending on the diversity of biological communities and their respective carbon utilisation pathways (Pancost & Sinninghe Damsté, 2003). Consequently, organic carbon isotopic trends can appear strongly decoupled from trends in carbonate carbon for primary biogeochemical and ecological reasons (e.g. Pancost *et al.*, 1998). The clear shifts in organic matter source contributions is evidenced by the notable variations in a wide range of lipid biomarker abundances through the Nafun Group of TM-6, particularly during the Shuram excursion. This underscores the biological richness underlying stratigraphic organic carbon isotope ratio data through the largest carbon isotope excursion in the geologic record.

If primary, the Shuram excursion provides an important isotope mass balance constraint on the middle to late Ediacaran carbon cycle. But in considering mechanisms for the excursion, it is useful to evaluate the quality of the assumptions commonly made in these interpretations. Most isotope mass balance frameworks for the geological carbon cycle make three assumptions (often implicitly) to solve for the burial fraction of organic carbon: steady state (where inputs and outputs are equal), the isotopic composition of the inputs and the isotopic difference between coeval carbonates and organic matter (Hayes *et al.*, 1999). Although dynamics are required by the excursion itself, the long timescales suggested by the substantial stratigraphic thickness of the Shuram excursion support quasi-static interpretations of the data (e.g. Rothman *et al.*, 2003). The isotopic composition of historical carbon cycle inputs cannot be directly observed and is often set between −5 and −7‰. But it is important to note that mantle carbon is highly variable and bimodal (one mode at −25‰ and another at −6‰) in its isotopic composition (Deines, 2002), nearly displaying the range observed in sedimentary rocks. In addition to the variable isotopic composition of outgassing, the likelihood of changes in the isotopic composition of the inputs is assured by the weathering of pre-existing sedimentary rocks (e.g. Halevy *et al.*, 2012). The Shuram excursion requires input values lower than −12‰. But values this low for historical carbon inputs are, in principle, reasonable. Isotopic differences between carbonates and organic carbon are often set between 25 and 30‰ and assumed to be constant. In principle, however, this difference (as $\Delta^{13}C_{carb\text{-}org}$) is observable in sedimentary rocks. As stated above, organic carbon isotope ratios need not record global trends. Nevertheless, several Shuram-age sections with paired records capture a secular increase in the observed $\Delta^{13}C_{carb\text{-}org}$ (e.g. Calver, 2000; Fike *et al.*, 2006; McFadden *et al.*, 2008), suggesting a need to interrogate a different hypothesis for the origin of this excursion – one wherein the $\delta^{13}C_{carb}$ values were largely controlled and driven by global changes in carbon isotope fractionations between coeval carbonate and organic carbon (e.g. Rothman *et al.*, 2003). Mass balance can be satisfied with multiple combinations of lower input values, reduced organic carbon burial fluxes and lower fractionations. But if the observed changes in $\Delta^{13}C_{carb\text{-}org}$ are indeed global in scope, mechanisms behind why these fractionations might change so systematically remain unclear.

CONCLUSIONS

Paired data sets of $\delta^{13}C_{carb}$ and $\delta^{13}C_{org}$ are largely decoupled during the Shuram excursion, even in highly organic-rich strata that characterise deeper-water paleoenvironments of the Nafun Group in Oman. Although the well-defined $\delta^{13}C_{carb}$ decline at the beginning of the Shuram excursion is not recorded in the carbon isotopic composition of any of the organic phases (TOC, bitumen, and kerogen), these materials show systematic trends that define a broad negative excursion, the onset of which occurs within the Khufai Formation and ends with a recovery that matches $\delta^{13}C_{carb}$ in the middle to upper Shuram Formation. Neither the carbon isotopic composition of the organic phases nor the difference between $\delta^{13}C_{carb}$ and $\delta^{13}C_{org}$ varies as a function of organic concentration. Lipid biomarker data reveal substantial changes in the biological communities and organic matter source inputs through the Shuram excursion in this sedimentary basin, but within the ranges expected of Neoproterozoic sedimentary rocks. Together these observations imply that carbonate–organic isotopic decoupling during the Shuram excursion is not a result of mixing of fossil or exogenous carbon sources (either DOC, detrital or migrated) with syngenetic organic matter, although differential mixing of distinct syngenetic sources may have played an important role in the observed differences between inorganic and organic carbon isotope ratios. Ultimately, these results highlight the possibility that systematic global changes in the fractionations between organic and inorganic carbon provided a driving mechanism for the Shuram excursion.

ACKNOWLEDGMENTS

We acknowledge the Agouron Institute for supporting this work, Petroleum Development Oman for access to subsurface materials and Kristin Bergmann for helpful comments. Additionally, we acknowledge editors Roger Buick and Kurt Konhauser for handling the manuscript and constructive comments provided by three anonymous reviewers.

REFERENCES

Ader M, Macouin M, Trindade RIF, Hadrien M-H, Yang Z, Sun Z, Besse J (2009) A multilayered water column in the Ediacaran Yangtze platform? Insights from carbonate and organic matter paired δ13C. *Earth and Planetary Science Letters* **288**, 213–227.

Allen PA (2007) The Huqf Supergroup of Oman: basin development and context for Neoproterozoic glaciation. *Earth-Science Reviews* **84**, 139–185.

Al-Marjeby A, Nash DF (1986) A summary of the geology and oil habitat of the Eastern Flank hydrocarbon province of South Oman. *Marine and Petroleum Geology* **3**, 306–314.

Amthor JE, Grotzinger JP, Schröder S, Bowring SA, Ramezani J, Martin MW, Matter A (2003) Extinction of *Cloudina* and *Namacalathus* at the Precambrian-Cambrian boundary in Oman. *Geology* **31**, 431–434.

Bazhenova OK, Arefiev OA (1996) Geochemical peculiarities of Precambrian source rocks in the East European Platform. *Organic Geochemistry* **25**, 341–351.

Bergmann KD, Zentmyer RA, Fischer WW (2011) The stratigraphic expression of a large negative carbon isotope excursion from the Ediacaran Johnnie Formation, Death Valley. *Precambrian Research* **188**, 45–56.

Berkner LV, Marshall LC (1965) On the origin and rise of oxygen concentration in the Earth's atmosphere. *Journal of Atmospheric Science* **22**, 225–261.

Bjerrum CJ, Canfield DE (2011) Towards a quantitative understanding of the late Neoproterozoic carbon cycle. *Proceedings of the National Academy of Sciences* **108**, 5542–5547.

Bowring SA, Grotzinger JP, Condon DJ, Ramezani J, Newhall MJ, Allen PA (2007) Geochronologic constraints on the chronostratigraphic framework of the Neoproterozoic Huqf Supergroup, Sultanate of Oman. *American Journal of Science* **307**, 1097–1145.

Bristow TF, Kennedy MJ (2008) Carbon isotope excursions and the oxidant budget of the Ediacaran atmosphere and ocean. *Geology* **36**, 863–866.

Burns SJ, Matter A (1993) Carbon isotopic record of the latest Proterozoic from Oman. *Eclogae Geologicae Helvetiae* **86**, 595–607.

Butterfield NJ, Grotzinger JP (2012) Palynology of the Huqf Supergroup, Oman. In: *Geology and Hydrocarbon Potential of Neoproterozoic-Cambrian Basins in Asia*, **Vol. 366** (eds Bhat GM, Thurow CJ, Thusu JW, Cozzi A). Geological Society, London, Special Publications. pp. 1–13.

Calver CR (2000) Isotope stratigraphy of the Ediacaran (Neoproterozoic III) of the Adelaide Rift Complex, Australia, and the overprint of water column stratification. *Precambrian Research* **100**, 121–150.

Cao C, Love GD, Hays LE, Wang W, Shen S, Summons RE (2009) Biogeochemical evidence for euxinic oceans and ecological disturbance presaging the end-Permian mass extinction event. *Earth and Planetary Science Letters* **281**, 188–201.

Close HG, Bovee R, Pearson A (2011) Inverse carbon isotope patterns of lipids and kerogen record heterogeneous primary biomass. *Geobiology* **9**, 250–265.

Cozzi A, Allen PA, Grotzinger JP (2004) Understanding carbonate ramp dynamics using $\delta^{13}C$ profiles: examples from the Neoproterozoic Buah Formation of Oman. *Terra Nova* **16**, 62–67.

Danovaro R, Dell'Anno A, Pusceddu A, Gambi C, Heiner I, Kristensen RM (2010) The first metazoan living in permanently anoxic conditions. *BMC Biology* **8**, 1–10.

Deines P (2002) The carbon isotope geochemistry of mantle xenoliths. *Earth-Science Reviews* **58**, 247–278.

Derry LA (2010a) A burial diagenesis origin for the Ediacaran Shuram-Wonoka carbon isotope anomaly. *Earth and Planetary Science Letters* **294**, 152–162.

Derry LA (2010b) On the significance of $\delta^{13}C$ correlations in ancient sediments. *Earth and Planetary Science Letters* **296**, 497–501.

Farrimond P, Talbot HM, Watson DF, Schulz LK, Wilhelms A (2004) Methylhopanoids: molecular indicators of ancient bacteria and a petroleum correlation tool. *Geochimica et Cosmochimica Acta* **68**, 3873–3882.

Fike DA (2007) Carbon and sulfur isotopic constraints on Ediacaran biogeochemical processes, Huqf Supergroup, Sultanate of Oman. PhD dissertation, Massachusetts Institute of Technology.

Fike DA, Grotzinger JP (2008) A paired sulfate-pyrite $\delta^{34}S$ approach to understanding the evolution of the Ediacaran-Cambrian sulfur cycle. *Geochimica et Cosmochimica Acta* **72**, 2636–2648.

Fike DA, Grotzinger JP, Pratt LM, Summons RE (2006) Oxidation of the Ediacaran Ocean. *Nature* **444**, 744–747.

Fowler MG, Douglas AG (1987) Saturated hydrocarbon biomarkers in oils of Late Precambrian age from Eastern Siberia. *Organic Geochemistry* **11**, 201–213.

Gorin GE, Racz LG, Walter MR (1982) Late Precambrian-Cambrian sediments of Huqf Group, Sultanate of Oman. *The American Association for Petroleum Geologists Bulletin* **60**, 2609–2627.

Grantham PJ, Wakefield LL (1988) Variations in the sterane carbon number distributions of marine source rock derived crude oils through geological time. *Organic Geochemistry* **12**, 61–74.

Grantham PJ, Lijmbach GWM, Posthuma J, Hughes Clarke MW, Willink RJ (1987) Origin of crude oils in Oman. *Journal of Petroleum Geology* **11**, 61–80.

Grosjean E, Love GD, Stalvies C, Fike DA, Summons RE (2009) Origin of petroleum in the Neoproterozoic-Cambrian South Oman Salt Basin. *Organic Geochemistry* **40**, 87–110.

Grotzinger JP, Al-Siyabi AH, Al-Hashimi RA, Cozzi A (2002) New model for the tectonic evolution of Neoproterozoic-Cambrian Huqf Supergroup basins, Oman. *GeoArabia* **7**, 241.

Grotzinger JP, Fike DA, Fischer WW (2011) Enigmatic origin of the largest-known carbon isotope excursion in Earth's history. *Nature Geoscience* **4**, 285–292.

Halevy I, Peters SE, Fischer WW (2012) Sulfate burial constraints on the Phanerozoic sulfur cycle. *Science* **337**, 331–334.

Hayes JM, Strauss H, Kaufman AJ (1999) The abundance of ^{13}C in marine organic matter and isotopic fractionation in the global biogeochemical cycle of carbon during the past 800 Ma. *Chemical Geology* **161**, 103–125.

Herron SL, Le Tendre L (1990) Wireline source-rock evaluation in the Paris Basin. In: *Deposition of Organic Facies*, **Vol. 30** (ed. Huc A). American Association of Petroleum Geologists, Tulsa, OK, Special Studies in Geology, pp. 57–71.

Hoffman PF, Kaufman AJ, Halverson GP, Schrag DP (1998) A Neoproterozoic Snowball Earth. *Science* **281**, 1342–1346.

Höld IM, Schouten S, Jellema J, Sinninghe Damsté JS (1999) Origin of free and bound mid-chain methyl alkanes in oils, bitumens and kerogens of the marine, Infracambrian Huqf Formation (Oman). *Organic Geochemistry* **30**, 1411–1428.

Jansyn J (1990) Strato-tectonic evolution of a large subsidence structure associated with the late Proterozoic Wonoka Formation at Wilpena Pound, central Flinders Ranges, South

Australia. B.Sc. Honours thesis, University of Adelaide (unpublished).
Jiang GQ, Wang X, Shi X, Xiao S, Zhang S, Dong J (2012) The origin of decoupled carbonate and organic carbon isotope signatures in the early Cambrian (*ca.* 542–520 Ma) Yangtze platform. *Earth and Planetary Science Letters* **317-318**, 96–110.
Johnston DT, Macdonald FA, Gill BC, Hoffman PF, Schrag DP (2012) Uncovering the Neoproterozoic carbon cycle. *Nature* **483**, 320–324.
van Kaam-Peters HME, Sinninghe Damsté JS (1997) Characterisation of an extremely organic sulfur-rich, 150 Ma carbonaceous rock: paleoenvironmental implications. *Organic Geochemistry* **27**, 371–397.
Kaufman AJ, Corsetti FA, Varni MA (2007) The effect of rising atmospheric oxygen on the carbon and sulfur isotope anomalies in the Neoproterozoic Johnnie Formation, Death Valley, USA. *Chemical Geology* **237**, 47–63.
Kelly AE (2009) Hydrocarbon biomarkers for biotic and environmental evolution through the Neoproterozoic-Cambrian transition. PhD dissertation, Massachusetts Institute of Technology.
Kelly AE, Love GD, Zumberge JE, Summons RE (2011) Hydrocarbon biomarkers of Neoproterozoic to Lower Cambrian oils from eastern Siberia. *Organic Geochemistry* **42**, 640–654.
King N, Westbrook MJ, Young SL, Kuo A, Abedin M, Chapman J, Fairclough S, Hellsten U, Isogai Y, Letunic I, Marr M, Pincus D, Putnam N, Rokas A, Wright KJ, Zuzow R, Dirks W, Good M, Goodstein D, Lemons D, Li W, Lyons JB, Morris A, Nichols S, Richter DJ, Salamov A, JGI Sequencing, Bork P, Lim WA, Manning G, Miller WT, McGinnis W, Shapiro H, Tjian R, Grigoriev IV, Rokhsar D (2008) The genome of choanoflagellate *Monosiga brevicollis* and the origin of metazoans. *Nature* **451**, 783–788.
Klomp UC (1986) The chemical structure of a pronounced series of iso-alkanes in South Oman crudes. *Organic Geochemistry* **10**, 807–814.
Knauth LP, Kennedy MJ (2009) The late Precambrian greening of the Earth. *Nature* **460**, 728–732.
Knoll AH, Carroll SB (1999) Early animal evolution: emerging views from comparative biology and geology. *Science* **284**, 2129–2137.
Knoll AH, Hayes JM, Kaufman AJ, Swett K, Lambert IB (1986) Secular variation in carbon isotope ratios from Upper Proterozoic successions of Svalbard and East Greenland. *Nature* **321**, 832–838.
Knoll AH, Summons RE, Waldbauer JR, Zumberge JE (2007) The geological succession of primary producers in the oceans. In: *The Evolution of Primary Producers in the Sea* (eds Falkowski P, Knoll AH). Elsevier, Burlington, pp. 133–163.
Le Guerroué E, Cozzi A (2010) Veracity of Neoproterozoic negative C-isotope values: the termination of the Shuram negative excursion. *Gondwana Research* **17**, 653–661.
Le Guerroué E, Allen PA, Cozzi A (2006a) Chemostratigraphic and sedimentological framework of the largest negative carbon isotopic excursion in Earth history: the Neoproterozoic Shuram Formation (Nafun Group, Oman). *Precambrian Research* **146**, 68–92.
Le Guerroué E, Allen PA, Cozzi A (2006b) Parasequence development in the Ediacaran Shuram Formation (Nafun Group, Oman): high resolution stratigraphic test for primary origin of negative carbon isotopic ratios. *Basin Research* **18**, 205–220.
Le Guerroué E, Allen PA, Cozzi A, Etienne JL, Fanning M (2006c) 50 Myr recovery from the largest $\delta^{13}C$ excursion in the Ediacaran ocean. *Terra Nova* **18**, 147–153.
Logan GA, Hayes JM, Hieshima GB, Summons RE (1995) Terminal Proterozoic reorganisation of biogeochemical cycles. *Nature* **376**, 53–56.
Loosveld RJH, Bell A, Terken JJM (1996) The tectonic evolution of interior Oman. *GeoArabia* **1**, 28–50.
Love GD, Stalvies C, Grosjean E, Meredith W, Snape CE (2008) Analysis of molecular biomarkers covalently bound within Neoproterozoic sedimentary kerogen. In: *From Evolution to Geobiology: Research Questions Driving Paleontology at the Start of a New Century*, **Vol. 4** (eds Kelley PH, Bambach RK). Paleontological Society, Yale University Printing & Publishing Services, New Haven, CT.
Love GD, Grosjean E, Stalvies C, Fike DA, Grotzinger JP, Bradley AS, Kelly AE, Bhatia M, Meredith W, Snape CE, Bowring SA, Condon DJ, Summons RE (2009) Fossil steroids record the appearance of Demospongiae during the Cryogenian Period. *Nature* **457**, 718–722.
Loyd SJ, Marenco PJ, Hagadorn JW, Lyons TW, Kaufman AJ, Sour-Tovar F, Corsetti FA (2013) Local $\delta^{34}S$ variability in ~580 Ma carbonates of northwestern Mexico and the Neoproterozoic marine sulfate reservoir. *Precambrian Research* **224**, 551–569.
Mann U, Leythaeuser D, Muller PJ (1986) Relation between source rock properties and wireline log parameters: an example from lower Jurassic Posidonia shale, NW Germany. *Advances in Organic Geochemistry* **10**, 1105–1112.
Marenco PJ, Corsetti FA, Hammond DE, Kaufman AJ, Bottjer DJ (2008) Oxidation of pyrite during extraction of carbonate associated sulfate. *Chemical Geology* **247**, 124–132.
McCarron GME (2000) The sedimentology and chemostratigraphy of the Nafun Group, Huqf Supergroup, Oman. PhD dissertation, Oxford University, pp. 175.
McFadden KA, Huang J, Chu X, Jiang G, Kaufman AJ, Zhou C, Yuan X, Xiao S (2008) Pulsed oxidation and biological evolution in the Ediacaran Doushantuo Formation. *Proceedings of the National Academy of Sciences* **105**, 3197–3202.
Melim LA, Swart PK, Eberli GP (2004) Mixing-zone diagenesis in the subsurface of Florida and the Bahamas. *Journal of Sedimentary Research* **74**, 904–913.
Meyer BL, Nederlof MH (1984) Identification of source rocks on wireline logs by density/resistivity and sonic transit time/resistivity crossplots. *American Association of Petroleum Geologists Bulletin* **68**, 121–129.
Nielsen C (2008) Six major steps in animal evolution: are we derived from sponge larvae? *Evolution and Development* **10**, 241–257.
Oehlert AM, Lamb-Wozniak KA, Devlin QB, Mackenzie GJ, Reijmer JJG, Swart PK (2012) The stable carbon isotopic composition of organic material in platform derived sediments: implications for reconstructing the global carbon cycle. *Sedimentology* **59**, 319–335.
Osburn MR, Grotzinger JP, Bergmann KD (2013) Facies, stratigraphy, and evolution of a middle Ediacaran carbonate ramp: Khufai Formation, Sultanate of Oman. *AAPG Bulletin. In press.*
Ostermann DR, Curry WB (2000) Calibration of stable isotopic data: an enriched $\delta^{18}O$ standard used for source gas mixing detection and correction. *Paleoceanography* **15**, 353–360.
Pancost RD, Sinninghe Damsté JS (2003) Carbon isotopic compositions of prokaryotic lipids as tracers of carbon cycling in diverse settings. *Chemical Geology* **195**, 29–58.
Pancost RD, Freeman KH, Patzkowsky ME, Wavrek D, Collister JW (1998) Molecular indicators of redox and marine phytoplankton composition in the late Middle Ordovician of Iowa, U.S.A. *Organic Geochemistry* **29**, 1649–1662.

Pell SD, McKirdy DM, Jansyn J, Jenkins RJF (1993) Ediacaran carbon isotope stratigraphy of South Australia. *Transactions of the Royal Society of South Australia* **117**, 153–161.

Peters KE, Walters CC, Moldowan JM (2005) *The Biomarker Guide*, 2nd edn. Cambridge University Press, Cambridge, pp. 1132.

Rohrssen M, Love GD, Fischer WW, Finnegan S, Fike DA (2013) Lipid biomarkers record fundamental changes in the microbial community structure of tropical seas during the Late Ordovician Hirnantian glaciation. *Geology* **41**, 127–130.

Rothman DH, Hayes JM, Summons RE (2003) Dynamics of the Neoproterozoic carbon cycle. *Proceedings of the National Academy of Sciences* **100**, 8124–8129.

Schrag DP, Higgins JA, Macdonald FA, Johnston DT (2013) Authigenic carbonate and the history of the global carbon cycle. *Science* **339**, 540–543.

Schröder S, Schreiber BC, Amthor JE, Matter A (2004) Stratigraphy and environmental conditions of the terminal Neoproterozoic-Cambrian period in Oman: evidence from sulfur isotopes. *Journal of the Geological Society London* **161**, 489–499.

Schwark L, Empt P (2006) Sterane biomarkers as indicators of Palaeozoic algal evolution and extinction events. *Palaeogeography, Palaeoclimatology, Palaeoecology* **240**, 225–236.

Scott KM, Schwedock J, Schrag DP, Cavanaugh CM (2004) Influence of Form IA RubisCO and environmental dissolved inorganic carbon on the 13C of the clam-chemoautotroph symbiosis *Solemya Velum*. *Environmental Microbiology* **6**, 1210–1219.

Scott C, Lyons TW, Bekker A, Shen Y, Poulton SW, Chu X, Anbar AD (2008) Tracing the stepwise oxygenation of the Proterozoic ocean. *Nature* **452**, 456–459.

Sperling EA, Laflamme M, Peterson KJ (2011) Rangeomorphs, *Thectardis* (Porifera?) and dissolved organic carbon in the Ediacaran oceans. *Geobiology* **9**, 24–33.

Summons RE, Jahnke LL, Logan GA, Hope JM (1999) 2-Methylhopanoids as biomarkers for cyanobacterial oxygenic photosynthesis. *Nature* **398**, 554–557.

Swanson-Hysell NL, Rose CV, Calmet CC, Halverson GP, Hurtgen MT, Maloof AC (2010) Cryogenian glaciation and the onset of carbon-isotope decoupling. *Science* **328**, 608–611.

Swart PK (2008) Global synchronous changes in the carbon isotopic composition of carbonate unrelated to changes in the global carbon cycle. *Proceedings of the National Academy of Sciences* **105**, 13741–13745.

Towe KM (1970) Oxygen-collagen priority and the early metazoan fossil record. *Proceedings of the National Academy of Sciences* **65**, 781–788.

Urlwin B, Ayliffe DJ, Jansyn J, McKirdy DM, Jenkins RJF, Gostin VA (1993) A $\delta^{13}C$ survey of carbonate in the Early Ediacaran Wonoka Formation. In: *Field guide to the Adelaide Geosyncline and Amadeus Basin, Australia* (eds Jenkins RJF, Lindsay JF, Walter MR). Record 1993/35. Australian Geological Survey Organisation, Canberra.

Volkman JK (1986) A review of sterol markers for marine and terrigenous organic-matter. *Organic Geochemistry* **9**, 83–99.

Welander PV, Coleman M, Sessions AL, Summons RE, Newman DK (2010) Identification of a methylase required for 2-methylhopanoid production and implications for the interpretation of sedimentary hopanes. *Proceedings of the National Academy of Sciences* **107**, 8537–8542.